J Seismol (2026) 30:1
https://doi.org/10.1007/s10950-025-10356-2

RESEARCH

Discrimination of seismic event near the North Korean nuclear test site (January-March 2022) using multi-station P/S spectral ratios

Bo-Han Wang · Lian-Feng Zhao · Xiao-Bi Xie · Xi He · Yong Zhao · Zhen-Xing Yao

Received: 23 September 2025 / Accepted: 22 December 2025

Abstract Between January and March 2022, fifteen shallow seismic events occurred near the Punggye-ri Nuclear Test Site in North Korea. These events raised concerns about their source nature, particularly in light of satellite observations suggesting renewed activity at the site. Here, we analyzed vertical-component seismograms recorded at 38 broadband stations with epicentral distances ranging from 70 to 600 km. Regional phases, Pn, Pg, Sn, and Lg, were used to calculate P/S spectral amplitude ratios. The network-averaged P/S-type spectral ratios were computed at a reference distance of 300 km to distinguish potential explosions from natural tectonic earthquakes. The spectral-ratio characteristics of all 15 shallow events closely align with those of tectonic earthquakes. The shallow events can be clearly separated from the underground-explosion population. Therefore, the 15 seismic events are likely to be natural tectonic earthquakes resulting from local stress imbalances.

Highlights

- Multi-station P/S spectral ratios were used to identify 15 small-magnitude events near the North Korean nuclear test site.
- The seismic events are characterized by tectonic earthquakes, which are discriminated from historical underground nuclear tests.

Keywords Nuclear monitoring · Seismic discrimination · Multi-station P/S spectral ratios · North Korean nuclear test site

Supplementary Information The online version contains supplementary material available at https://doi.org/10.1007/s10950-025-10356-2.

B.-H. Wang · L.-F. Zhao (✉) · X. He · Z.-X. Yao
Key Laboratory of Planetary Science and Frontier Technology, Institute of Geology and Geophysics, Chinese Academy of Sciences, 19 Beituchengxilu, Chaoyang District, Beijing 100029, China
e-mail: zhaolf@mail.iggcas.ac.cn

B.-H. Wang
College of Earth and Planetary Sciences, University of Chinese Academy of Sciences, Beijing, China

L.-F. Zhao
Heilongjiang Mohe Observatory of Geophysics, Institute of Geology and Geophysics, Chinese Academy of Sciences, Beijing, China

L.-F. Zhao · Y. Zhao
Earthquake Networks Center, Beijing, China

X.-B. Xie
Institute of Geophysics and Planetary Physics, University of California at Santa Cruz, Santa Cruz, CA, USA

1 Introduction

Between January and March 2022, 15 earthquakes with magnitudes ranging from ML 2.1 to 3.7 occurred around the North Korean nuclear test site. According to the China Earthquake Data Center, these events were spatially and temporally close to the North

Published online: 17 January 2026

Korean nuclear test site, with up to 4 events occurring on the same day (Fig. S1). The nuclear test site was decommissioned in 2018 following the six North Korean nuclear tests, but there were reports of its reconstruction in early 2022. Satellite imagery indicates possible excavation activity at the site and newly constructed buildings in the main support areas adjacent to the facility (Fig. S2). Previous studies have paid significant attention to the impact of nuclear tests and related seismic activities in this region (Tibi 2021; Yao et al. 2018). Therefore, it's critical to identify the 15 recorded events as explosions, explosion-induced collapse, or tectonic earthquakes based on the relevant observations.

On October 6, 2006, North Korea conducted its first underground nuclear test, which generated seismic waves detected worldwide. However, the test's low yield and low seismic energy release complicate event discrimination. Kim and Richards (2007) used the P-wave/S-wave amplitude ratio at various frequencies as a discriminant to identify the seismic event as an underground nuclear explosion. Zhao et al. (2008) enhanced the single-station method by analyzing extensive regional seismic-phase data from Northeast China and incorporating site-effect and geometric spreading corrections and amplitude stacking. This approach extended the technique to a multi-station method, thereby broadening its applicability across a broader range of frequency bands. Furthermore, clear distinctions in seismic source characteristics were identified by comparing P/S spectral ratios (Pg/Lg, Pn/Lg, and Pn/Sn) between the DPRK's declared nuclear test and four nearby natural earthquakes. Following the initial 2006 test, North Korea conducted five additional nuclear tests in 2009, 2013, January and September 2016, and 2017. By the time of the 2016 tests, seismic methods for distinguishing nuclear explosions in North Korea had been widely implemented, including techniques such as P/S spectral ratios, relative relocation analysis, and source mechanism characterization. (Wen and Long 2010; Yang et al. 2021; Zhang and Wen 2014; Zhao et al. 2016, 2017, 2012, 2014). On September 3, 2017, during its sixth nuclear test, a collapse occurred minutes later, followed by 13 seismic events over the next seven months (Kim et al. 2018; Schaff et al. 2018; Walter et al. 2018). Pan et al. (2007) demonstrated the effectiveness of the P/S spectral ratio method even for low-yield explosions (Zhang et al. 2022). On 11 February 2022, an ML 3.7 earthquake (event 20220211) near the Punggye-ri nuclear test site in North Korea sparked interest in several studies (Ding et al. 2023; Kintner et al. 2024; Wang et al. 2023, 2024). However, fourteen other seismic events that occurred in close spatial and temporal proximity between January and March 2022 have not yet been examined (Fig. 1 and Table 1).

Several studies explored the source characteristics of the 20220211 event using various spectral and waveform-based methods. Wang et al. (2023) conducted precise event relocation, estimated its source depth at approximately 5.5 km, analyzed initial seismic phases, and compared P/S amplitude ratios. Their analysis conclusively identified the event as a natural tectonic earthquake rather than a nuclear explosion. Ding et al. (2023) enhanced this understanding by applying a modified Magnitude and Distance Amplitude Correction (MDAC) method to examine the spectral ratios of Pg/Lg and Pn/Lg. Their results demonstrated spectral characteristics consistent with those of historical tectonic earthquakes, distinctly different from those of explosion signatures. Complementing these findings, Kintner et al. (2024) employed regional coda spectral ratio analysis, which revealed significant differences in high-frequency S-wave energy between event 20220211 and known explosive sources, thereby reinforcing its tectonic origin.

Although previous studies have examined the 20220211 event, fourteen spatially and temporally related seismic events in its vicinity remain unexplored. The collective characteristics and underlying mechanisms of this group of events remain unclear and require further investigation. This study collected vertical-component seismic data primarily recorded by the regional seismic network in northeastern China. After extracting regional seismic phases from these datasets, we computed P/S spectral ratios and applied a multi-station approach to classify all 15 seismic events.

2 Data and method

We collected broadband vertical-component seismic data from the China National Digital Seismic Network (CNDSN), the Global Seismic Network (GSN), and the International Federation of Digital Seismograph Networks (FDSN) to construct a

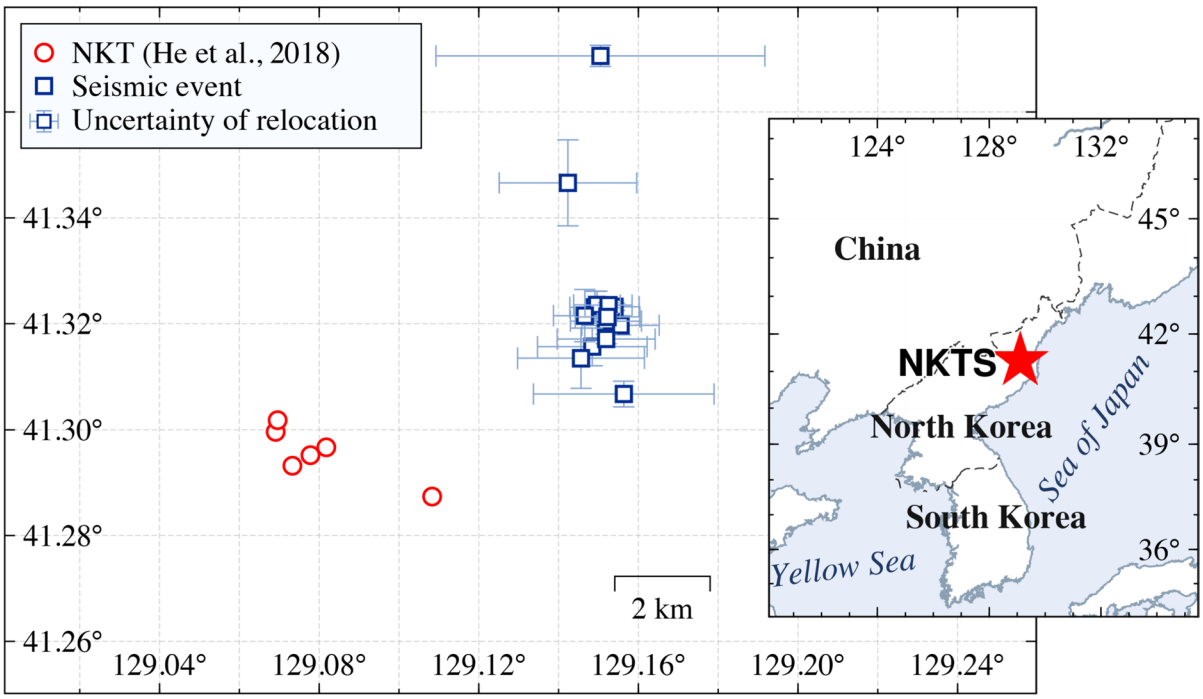

Fig. 1 Map showing spatial distribution of seismic events (blue square) and North Korean nuclear tests (red circle) (He et al. 2018). The error bars represent the uncertainties of the relocated events. The inset map shows the location of the North Korean nuclear test site (NKTS)

Table 1 List of the seismic events

Number	Date	Origin Time	Latitude (°N)	Longitude (°E)	Depth(m)	Magnitude(Ms)
1	2022–01–22	06:54:11	41.3467	129.1423	1.98	3.17 ± 0.22
2	2022–01–22	09:28:41	41.3201	129.1549	1.74	3.02 ± 0.38
3	2022–01–22	09:33:20	41.3913	129.1420	2.23	2.33 + 0.57
4	2022–01–23	12:46:04	41.3706	129.1505	1.81	2.34 ± 0.67
5	2022–02–11	01:35:24	41.3202	129.1524	1.87	2.71 ± 0.46
6	2022–02–13	22:15:15	41.3064	129.1568	1.85	2.65 ± 0.27
7	2022–02–13	22:23:51	41.3231	129.1490	2.15	2.51 ± 0.29
8	2022–02–14	05:33:21	41.3161	129.1479	1.97	2.35 ± 0.25
9	2022–02–14	10:47:26	41.3229	129.1542	2.20	2.56 ± 0.45
10	2022–02–18	02:45:00	41.3235	129.1496	1.90	2.85 ± 0.55
11	2022–02–18	03:38:20	41.3214	129.1472	1.91	2.45 ± 1.08
12	2022–02–22	21:07:07	41.3136	129.1454	2.15	2.39 ± 0.48
13	2022–02–28	12:22:50	41.3170	129.1521	2.01	2.55 ± 0.22
14	2022–03-03	17:15:26	41.3236	129.1521	2.21	2.88 ± 0.82
15	2022–03–11	17:49:18	41.3213	129.1522	1.85	2.26 ± 0.25

dataset for identifying seismic events near the North Korean nuclear test site. The dataset focuses on events occurring between January and March 2022, a period marked by significantly elevated seismic activity in the region (Fig. 2). Most of the stations used in this study are located in Northeast China,

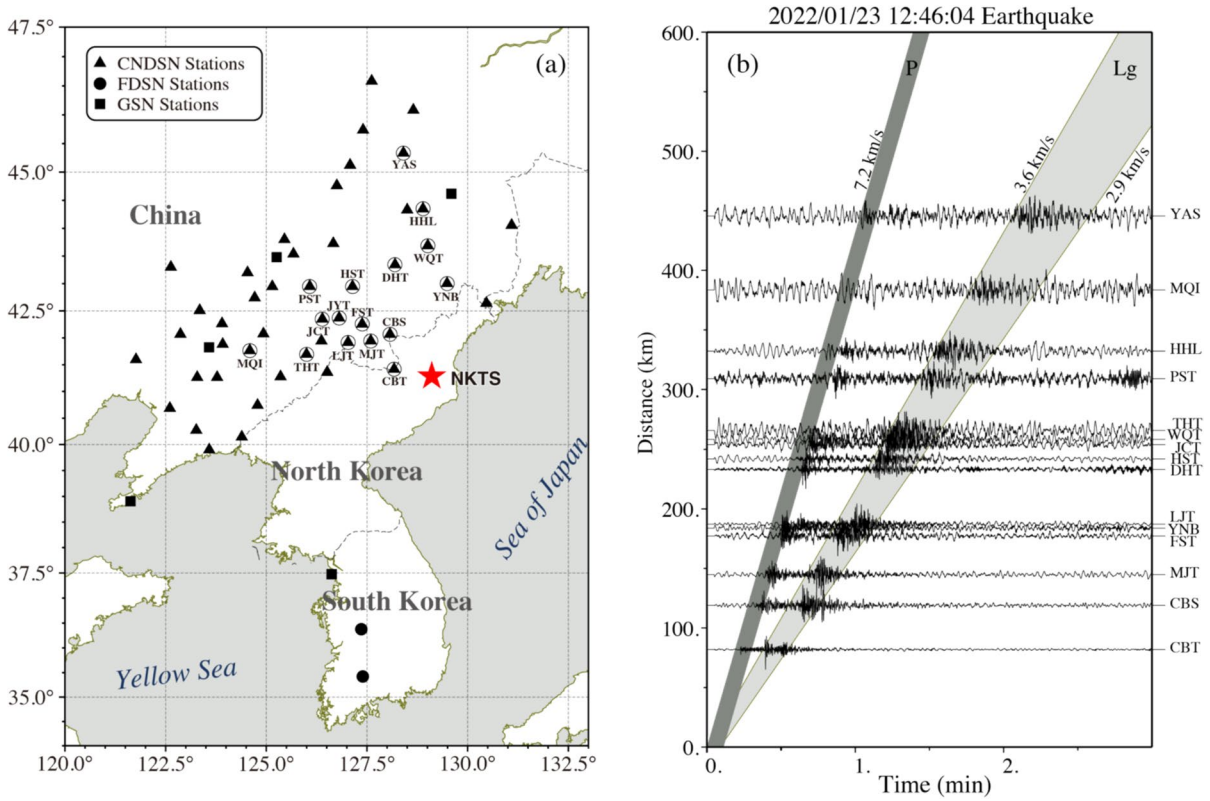

Fig. 2 **a** Map of seismograph station locations. CNDSN stations are marked with black solid triangles, FDSN stations are marked with black solid circles, and GSN stations are marked with black solid squares. The location of the North Korean test site (NKTS) is marked with a red star. Stations used in the waveform example shown in (b) are circled. **b** Normalized vertical-component velocity seismograms of the January 23, 2022, 12:46:04 UTC event. Waveforms are plotted by epicentral distance, with theoretical group velocity windows for P and Lg waves shaded in gray. The bandpass filter is 0.5–5.0 Hz

at epicentral distances ranging from 70 to 600 km from the test site, capturing clear regional seismic signals suitable for discrimination.

We used the PickNet deep learning model to pick P- and S-wave onsets and performed relocation using HypoDD (Waldhauser and Ellsworth 2000; Wang et al. 2019). The original event parameters were obtained from the China Earthquake Networks Center (CENC). The surface-wave magnitudes (Ms) were computed using the regional variable-period method adopted by Bonner et al. (2008), ensuring consistency with previous studies in Northeast Asia.

We selected 317 vertical-component records from 38 stations that met the criteria of epicentral distances between 70 and 600 km and a signal-to-noise ratio (SNR) greater than 2.0 (Fig. S3). These records contain abundant high-quality regional phases, including Pn, Pg, Sn, and Lg waves. Pn-waves are picked using a velocity window of 7.8–6.4 km/s, Pg-waves with 6.3–5.1 km/s, Sn-waves with 4.6–4.0 km/s, and Lg-waves with 3.7–2.9 km/s (Figs. 3a-c). Phase picking was conducted with a time-distance window and refined through manual inspection of waveform quality.

To discriminate between tectonic earthquakes and potential explosion-type events, we applied a multi-station P/S spectral-ratio method based on regional phase amplitude spectra, which is stable for both large and small magnitudes (He et al. 2018; Song et al. 2022; Zhang et al. 2022). P/S spectral ratios effectively discriminate between explosions and natural earthquakes by leveraging fundamental differences in their source physics. Explosions, which primarily produce compressional P-waves, are typically isotropic. In contrast, tectonic earthquakes generally result from double-couple faulting

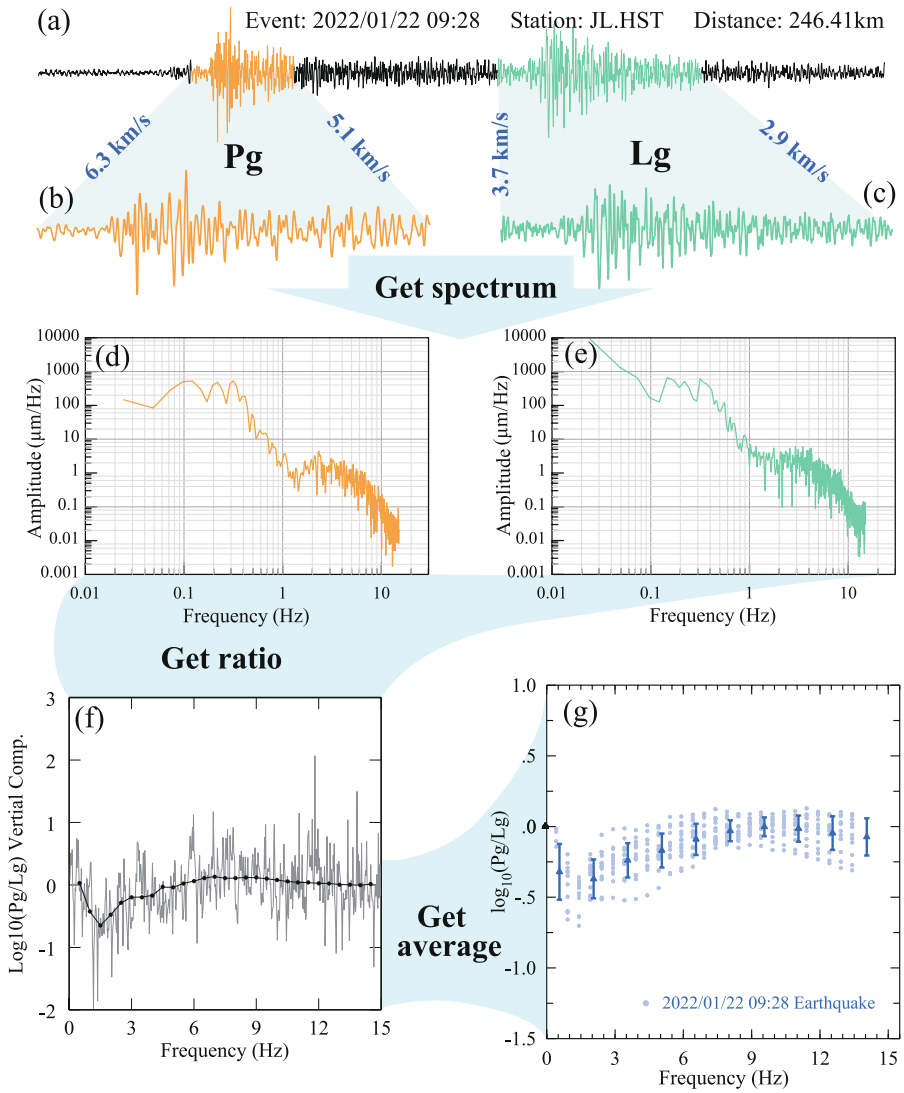

Fig. 3 An example of the Pg/Lg spectral amplitude ratio calculation. **a** Vertical-component seismograms from the 22 Jan 2022 seismic event recorded at station JL.HST, where two different velocity windows sampled the Pg signals (orange) and Lg signals (green). **b**, **c** Enlarged waveforms of the Pg and Lg signals. **d**, **e** Pg and Lg spectra. **f** Single-station Pg/Lg spectral ratio at JL.HST. The gray curve shows the unsmoothed raw ratio, and the black curve indicates the smoothed spectral ratio calculated using the integration-based method described in the text. **g** Network-averaged Pg/Lg spectral ratio for the event after distance normalization and residual correction

along fault planes and radiate most of their energy through shear waves. Consequently, explosions tend to exhibit higher P/S amplitude spectral ratios compared to natural earthquakes. Mathematically, the single-station P/S amplitude spectral ratio can be expressed as

$$A_{\mathrm{P/S}}(f_c) = \frac{\int_{f_c/\sqrt{2}}^{\sqrt{2}f_c} A_P(f)\mathrm{d}f}{\int_{f_c/\sqrt{2}}^{\sqrt{2}f_c} A_S(f)\mathrm{d}f} \tag{1}$$

where $A_{\mathrm{P/S}}(f_c)$ denotes the amplitude spectral ratio at the central frequency f_c, $A_P(f)$ represents the spectrum of P-wave phases (e.g., Pn, Pg), and $A_S(f)$ represents the spectrum of S-wave phases (e.g., Sn, Lg). f_c was varied from 0.5 Hz to 14.5 Hz, stepped in 0.5 Hz increments (Fig. 3f). We use the log-averaged spectral ratio as a smoothed measure, with the smoothing frequency band taken between $f_c/\sqrt{2}$ to $\sqrt{2}f_c$ (Bowman and Kennett 1991; Hartse et al. 1997; Richards and Kim 2007; Yang 2002; Zhao et al. 2008). The spectral ratio calculation process is illustrated in Fig. 3.

To obtain reliable network-averaged spectral ratios that reflect source characteristics, we applied corrections to the single-station spectral ratios. For each frequency f_c, the observed spectral ratios $A_{\mathrm{ij}}(f_c)$ between

event i and station j were converted to logarithmic form, and the corresponding hypocentral distances R_{ij} can be expressed as $\log R_{ij}$. A linear distance-decay model was obtained by fitting in the logarithmic domain:

$$\log A_{ij}(f_c) = a(f_c) + b(f_c) log R_{ij} + \varepsilon_{ij}(f_c) \quad (2)$$

where $a(f_c)$ and $b(f_c)$ are the intercept and attenuation slope determined by liner regression, and $\varepsilon_{ij}(f_c)$ is the regression residual. The regression used all available station observations at each frequency to obtain the attenuation coefficient $b(f_c)$ and intercept $a(f_c)$. All observations were then normalized to a reference distance R_0 of 300 km by subtracting the distance-dependent term derived from the regression:

$$\log A_{ij}^{corr}(f_c) = \log A_{ij}(f_c) + (\log R_0 - \log R_{ij}) b(f_c) \quad (3)$$

After this distance correction, most of the remaining variability among stations for a given event is attributable to near-surface or site effects, since the source and path terms have mainly been removed.

To further remove these site effects, we calculated event-mean spectra and defined event residuals as the deviation of each record from its corresponding event mean (Hartse et al. 1997):

$$r_{ij}(f_c) = \log A_{ij}^{corr}(f_c) - \langle \log A_{i}^{corr}(f_c) \rangle \quad (4)$$

These residuals quantify the relative amplification or deamplification of each station relative to the event average. By averaging the residuals from each station across multiple events, we obtained the frequency-dependent station (basement) response, which represents the stable amplification pattern at each site. We then subtracted this station response from all normalized observations, yielding spectral ratios corrected for both distance attenuation and site amplification. This two-step correction effectively isolates the source radiation characteristics and allows robust averaging across the network (Fig. S4).

3 Result

We calculated spectral ratios (Figs. 4a–c) for six historical nuclear tests, five earthquakes, and the fifteen seismic events occurring between January and March 2022 at the Punggye-ri Nuclear Test Site (Tables S1 and S2). The result demonstrates that the spectral ratios of the 15 recent events closely resemble those of the historical earthquakes. Network-averaged spectral ratios (Pg/Lg, Pn/Lg, and Pn/Sn) of the 15 events from 2022 were compared against those from North Korea's historical nuclear tests (Figs. 4a–c). The spectral ratios for all 15 events lie clearly below zero and are distinctly separated from the explosion data.

Two distinct reference curves were derived by averaging the amplitude spectral ratios observed for historical nuclear tests and earthquakes to aid source-type discrimination (Figs. 4d–f). These reference curves highlight significant spectral ratio differences between explosion and earthquake sources. Figures 4d–f show complete separation between explosion and earthquake groups for Pg/Lg, Pn/Lg, and Pn/Sn spectral ratios at frequencies above 2.0 Hz, confirming that network-averaged spectral ratios robustly discriminate tectonic from explosive sources (He et al. 2018; Zhao et al. 2016, 2008, 2014).

4 Discussion and conclusions

In this study, we analyzed the P/S amplitude spectral ratios of 15 seismic events. We found that their spectral and waveform characteristics are consistent with regional tectonic earthquakes, suggesting tectonic sources rather than explosions. In addition, the waveform characteristics also support this conclusion. The observed waveforms show clear arrivals of S-wave phases such as Sn and Lg (Fig. 2b), which are more typical of tectonic earthquakes than explosions (Fig. S5). The waveform characteristics of these events are more similar to those of typical tectonic earthquakes.

The P/S amplitude spectral ratio is a crucial indicator for distinguishing between explosions and earthquakes. Explosive sources typically produce higher P/S ratios due to the much greater energy carried by P-waves relative to S-waves. In contrast, tectonic earthquakes usually generate lower P/S ratios because S-wave energy is relatively stronger. All 15 events in this study exhibited low P/S spectral ratios, suggesting a tectonic source. As future work, we will use explosion source-spectrum models (Jin et al. 2024) to derive equivalent P/S spectral ratios for smaller-yield explosions near NKTS.

Wang et al. (2023) found that the 11 February 2022 event was a tectonic earthquake (M_L 3.7)

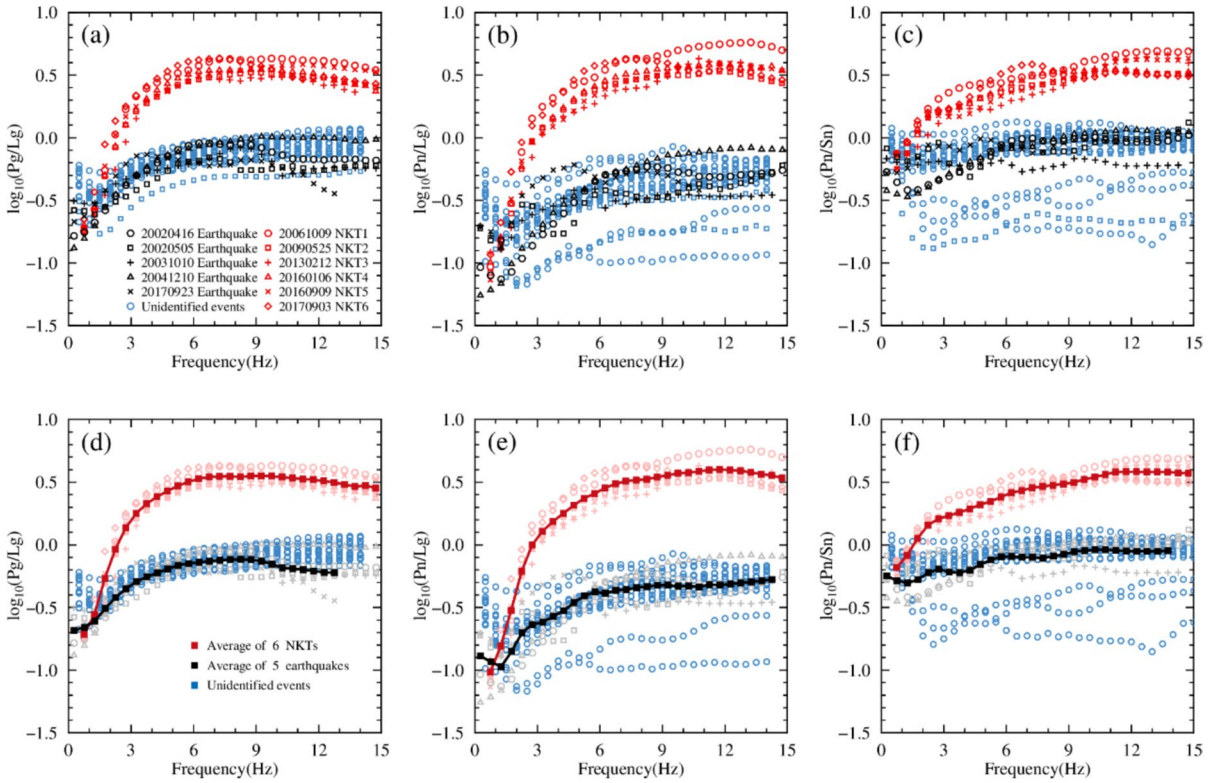

Fig. 4 Spectral ratios for underground nuclear tests (red symbols), nearby natural earthquakes (black symbols), and unidentified events (blue symbols). **a-c** Comparison of network average amplitude spectral ratios of Pg/Lg, Pn/Lg, and Pn/Sn for six underground nuclear tests (red), nearby natural earthquake events (black), and unidentified events (blue). **d-f** Light red symbols represent network average amplitude spectral ratios for individual underground nuclear tests, light gray symbols for individual natural earthquake events, and blue symbols for unidentified events. Solid symbols represent the averages for six underground nuclear tests (red) and five natural earthquake events (black)

located approximately 6.6 km from the tunnels at the Punggye-ri nuclear test site. Kintner et al. (2024) used a coda-wave amplitude ratio-based source discrimination model, and also classified the 20220211 event as tectonic. Our results are consistent with both studies. We expanded the analysis to include 15 seismic events that occurred in the same region over a similar period. Using a unified P/S spectral-ratio discrimination approach, we analyzed the source characteristics of this event sequence to determine whether they reflect a consistent tectonic source or are influenced by anthropogenic factors.

Although this study did not obtain direct focal mechanism solutions, the spatiotemporal clustering of these events (Fig. 1) suggests that they may be related to localized stress perturbations caused by underground activities at the nuclear test site. Such perturbations may originate from small-scale blasting during tunnel excavation, maintenance, or clearing operations, potentially leading to minor collapses and subsequent stress release.

Acknowledgements The comments from Editor Angela Saraò and three anonymous reviewers are valuable and greatly improved this manuscript. This research was supported by the National Natural Science Foundation of China (Grant Nos. 42430306 and U2139206).

Author contribution B.-H.W. and L.-F.Z. wrote the main manuscript text. Y.Z. collected the data. All authors reviewed the manuscript.

Funding National Natural Science Foundation of China,42430306,U2139206

Data availability Waveform data used in this study were primarily obtained from the China Earthquake Data Center. Additional waveform and station metadata were downloaded

using Obspy (Krischer et al. 2015) through the web services of the International Federation of Digital Seismograph Networks (FDSN), provided by the Incorporated Research Institutions for Seismology Data Management Center (IRIS DMC) at http://www.iris.edu/ds/nodes/dmc/ (last accessed July 2025). Certain figures were generated using Generic Mapping Tools (GMT) at https://www.generic-mapping-tools.org/ (last accessed July 2025) (Wessel et al. 2019).

Declarations

Conflict interests The authors declare no competing interests.

References

Bonner J, Herrmann RB, Harkrider D, Pasyanos M (2008) The surface wave magnitude for the 9 October 2006 North Korean nuclear explosion. Bull Seismol Soc Am 98(5):2498–2506

Bowman JR, Kennett BLN (1991) Propagation of Lg waves in the North Australian Craton: influence of crustal velocity gradients. Bull Seismol Soc Am 81(2):592–610

Ding S, Wang H, Zhu H, Xu H, Xu X (2023) Discrimination of seismic events in the North Korean Test Site and surrounding area using MDAC spectral ratio. Bull Seismol Soc Am 114(2):1140–1150

Hartse HE, Taylor SR, Phillips WS, Randall GE (1997) A preliminary study of regional seismic discrimination in central Asia with emphasis on western China. Bull Seismol Soc Am 87(3):551–568

He X, Zhao LF, Xie XB, Yao ZX (2018) High-precision relocation and event discrimination for the 3 September 2017 underground nuclear explosion and subsequent seismic events at the North Korean Test Site. Seismol Res Lett 89(6):2042–2048

Jin P, Xu HL, Ding SB, Wang WP, Zhu HF (2024) Source spectra of Pg and Lg waves from North Korean nuclear tests estimated using a nonmodel-based approach. Bull Seismol Soc Am 114(2):1151–1166

Kim WY, Richards PG (2007) North Korean nuclear test: seismic discrimination low yield. Eos Trans Am Geophys Union 88(14):158–161

Kim WY, Richards PG, Schaff D, Jo E, Ryoo Y (2018) Identification of seismic events on and near the North Korean Test Site after the underground nuclear test explosion of 3 September 2017. Seismol Res Lett 89(6):2120–2130

Kintner JA, Delbridge B, Alfaro-Diaz R, Scott Phillips W (2024) Seismic discrimination using regional distance coda-wave ratios. Seismol Res Lett 96(2A):1073–1087

Krischer L, Megies T, Barsch R, Beyreuther M, Lecocq T, Caudron C, Wassermann J (2015) ObsPy: a bridge for seismology into the scientific Python ecosystem. Comput Sci Discov 8(1):014003

Pan C, Jin P, Wang H (2007) Applicability of P/S amplitude ratios for the discrimination of low magnitude seismic events. Acta Seismol Sin 20(5):553–561

Richards PG, Kim W-Y (2007) Seismic signature. Nat Phys 3(1):4–6

Schaff DP, Kim WY, Richards PG, Jo E, Ryoo Y (2018) Using waveform cross correlation for detection, location, and identification of aftershocks of the 2017 nuclear explosion at the North Korea test site. Seismol Res Lett 89(6):2113–2119

Song Y, Zhao L-F, Xie X-B, Ma X, Du G, Tian X, Yao Z-X (2022) Seismological observations on the 2019 March 21 accidental explosion at Xiangshui chemical plant in Jiangsu, China. Geophys J Int 228(1):538–550

Tibi R (2021) Discrimination of seismic events (2006–2020) in North Korea using P/Lg amplitude ratios from regional stations and a bivariate discriminant function. Seismol Res Lett 92(4):2399–2409

Waldhauser F, Ellsworth WL (2000) A double-difference earthquake location algorithm: method and application to the northern Hayward fault, California. Bull Seismol Soc Am 90(6):1353–1368

Walter WR, Dodge DA, Ichinose G, Myers SC, Pasyanos ME, Ford SR (2018) Body-Wave methods of distinguishing between explosions, collapses, and earthquakes: application to recent events in North Korea. Seismol Res Lett 89(6):2131–2138

Wang J, Xiao ZW, Liu C, Zhao DP, Yao ZX (2019) Deep learning for picking seismic arrival times. J Geophys Res Solid Earth 124(7):6612–6624

Wang HC, Xu HL, Xu X, Zhu HF, Ding SB, Wang WP, Wang PZ (2023) Explosion or tectonic earthquake? Evidence that an ML 3.7 seismic event occurred near North Korea's nuclear test site on 11 February 2022. Seismol Res Lett 94(3):1334–1341

Wang T, Bian Y, You Q, Ren M, Yang Q (2024) Classification study of earthquakes and explosions in North Korea and adjacent regions. Seismol Res Lett 96(1):421–434

Wen L, Long H (2010) High-precision location of North Korea's 2009 nuclear test. Seismol Res Lett 81(1):26–29

Wessel P, Luis JF, Uieda L, Scharroo R, Wobbe F, Smith WHF, Tian D (2019) The generic mapping tools version 6. Geochem Geophys Geosyst 20(11):5556–5564

Yang XN (2002) A numerical investigation of geometrical spreading. Bull Seismol Soc Am 92(8):3067–3079

Yang G, Zhao LF, Xie XB, Zhang L, Yao ZX (2021) High-precision relocation with the burial depths of the North Korean underground nuclear explosions by combining Pn and Pg differential traveltimes. J Geophys Res Solid Earth 126(6):e2020JB020745

Yao J, Tian D, Lu Z, Sun L, Wen L (2018) Triggered seismicity after North Korea's 3 September 2017 nuclear test. Seismol Res Lett 89(6):2085–2093

Zhang M, Wen L (2014) Seismological evidence for a low-yield nuclear test on 12 May 2010 in North Korea. Seismol Res Lett 86(1):138–145

Zhang L, Zhao LF, Xie XB, He X, Yao ZX (2022) Yield estimation and event discrimination of the 4 August 2020 Beirut chemical explosion. Seismol Res Lett 93(4):2004–2014

Zhao L-F, Xie X-B, Wang W-M, Yao Z-X (2008) Regional seismic characteristics of the 9 October 2006 North Korean nuclear test. Bull Seismol Soc Am 98(6):2571–2589

Zhao L-F, Xie XB, Wang WM, Yao ZX (2012) Yield estimation of the 25 May 2009 North Korean nuclear explosion. Bull Seismol Soc Am 102(2):467–478

Zhao L-F, Xie XB, Wang WM, Yao ZX (2014) The 12 February 2013 North Korean underground nuclear test. Seismol Res Lett 85(1):130–134

Zhao L-F, Xie X-B, Wang W-M, Hao J-L, Yao Z-X (2016) Seismological investigation of the 2016 January 6 North Korean underground nuclear test. Geophys J Int 206(3):1487–1491

Zhao L-F, Xie XB, Wang WM, Fan N, Zhao X, Yao ZX (2017) The 9 September 2016 North Korean underground nuclear test. Bull Seismol Soc Am 107(6):3044–3051